



Lawrence Berkeley Laboratory

UNIVERSITY OF CALIFORNIA

Materials & Molecular Research Division

Submitted to Physical Review B

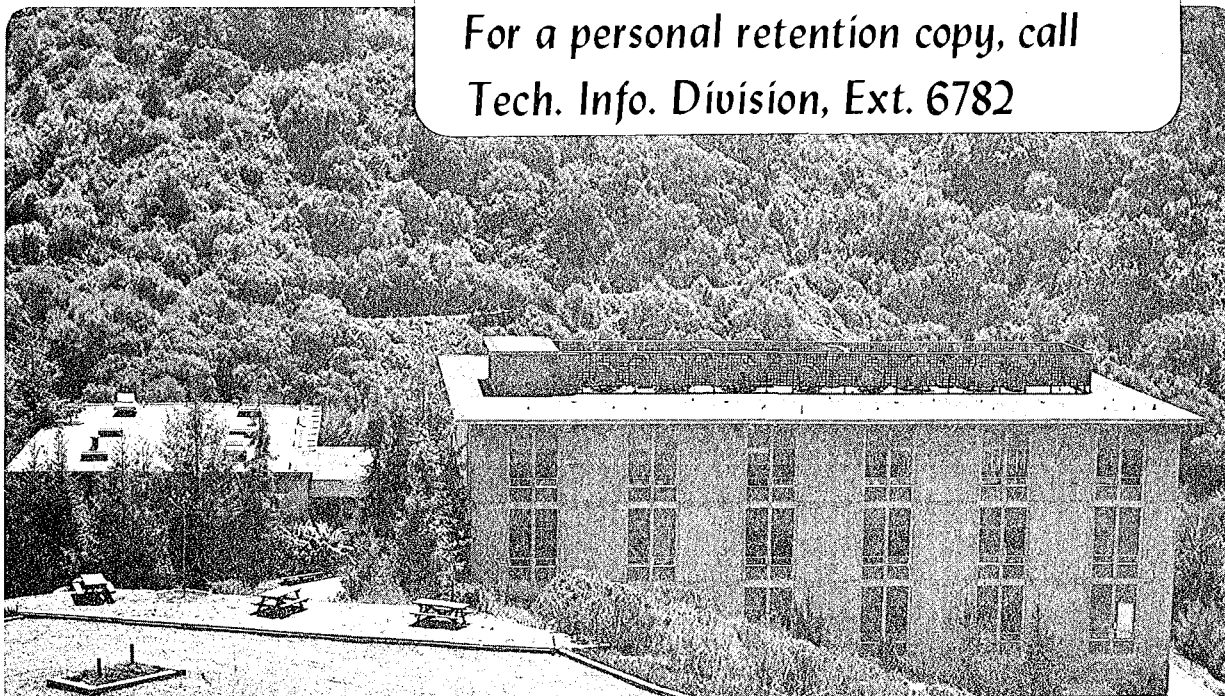
TEMPERATURE DEPENDENCE OF NORMAL EMISSION PHOTOELECTRON
DIFFRACTION AND ANALOGIES WITH EXAFS

S.D. Kevan, J.G. Tobin, D.H. Rosenblatt,
R.F. Davis, and D.A. Shirley

July 1980

TWO-WEEK LOAN COPY

*This is a Library Circulating Copy
which may be borrowed for two weeks.
For a personal retention copy, call
Tech. Info. Division, Ext. 6782*



LBL-11199
c.2

Temperature Dependence of Normal Emission Photoelectron
Diffraction and Analogies with EXAFS

S.D. Kevan, J.G. Tobin, D.H. Rosenblatt,
R.F. Davis, and D.A. Shirley

Materials and Molecular Research Division
Lawrence Berkeley Laboratory
and
Department of Chemistry
University of California
Berkeley, California 94720

July 1980

ABSTRACT

The temperature dependence of normal emission photoelectron diffraction (NPD) of the prototype adsorbate-substrate system Se-Ni(001) was studied. Two interesting observations emerged. Thermal diffuse scattering yielded a decreasing peak/valley contrast ratio in NPD with increasing temperature, characterized by an effective temperature $\theta_{\text{eff}} \sim 135\text{K}$. Also, a new low-temperature form of p(2x2) selenium structure was observed, with d_1 estimated to be larger by $\sim (0.06-0.1)\text{\AA}$ than the room-temperature form. The new form, which is probably undissociated H_2Se , is apparent through a systematic NPD peak shift reminiscent of EXAFS spectra. It is noted that NPD, though usually associated with LEED, in fact has strong similarities to EXAFS. This is particularly evident in the importance of an extended k-space data set and in the temperature sensitivity.

I. Introduction

In 1974, Liebsch proposed that surface structural studies on adsorbate covered clean surfaces similar to low energy electron diffraction (LEED) might be advantageously carried out using photoelectrons.¹ The relation of the angle-resolved photoemission (ARP) final state to a LEED state has long been recognized,²⁻⁴ and various theories dependent on LEED formalisms have been developed to treat photoelectron diffraction (PD) data.⁴⁻⁶ In addition, several experiments have been reported which have generally confirmed Liebsch's initial hypothesis concerning the structural sensitivity of PD.⁷⁻¹⁰ Our group has addressed the characterization of normal emission photoelectron diffraction (NPD), in which the photoemission intensity of an adsorbate core level is measured normal to the surface as a function of photon (and thus kinetic) energy.⁷ In NPD, an intensity-energy curve similar to a LEED I-V curve is generated which, when compared to theoretical curves, may yield a surface structure. Given its genesis, PD is usually conceptualized by its relation to LEED, and the same general accuracies and limitations are usually perceived to be associated with the two methods.

In this paper, we take the view that while this comparison to LEED is valuable, an equally enlightening comparison of normal photoelectron diffraction to extended x-ray absorption fine structure^{11,12}

(EXAFS) can be drawn. The important point is that the initial step in PD and surface EXAFS--an excitation of an electron localized in an adsorbate core level--is the same, while the details of the final state scattering in PD are best described by their relation to LEED. The fact that the electron source in PD is localized as in EXAFS implies that it is a phase-coherent process: the phase of the wave leaving the absorbing atom is fixed for each energy. A direct result of this is PD's ability to deal with disordered overlayers not normally accessible with LEED.^{7,9} Specializing to NPD, we note that, while the NPD intensity-energy curves resemble LEED I-V curves, their calculated behavior actually mimics EXAFS data, with d_{\perp} , the interplanar spacing between the overlayer and the outermost substrate layer, being the important structural parameter, rather than the nearest neighbor distance, R_{nn} . This result, first observed by Li and Tong¹³ and emphasized elsewhere,^{7,8} is illustrated in Figure 1. In the top three curves, the calculated selenium 3d normal emission ARP intensity for the p(2x2) Se-Ni(001) system is plotted for three different values of d_{\perp} . The oscillation frequency is seen to increase monotonically with d_{\perp} in much the same way as EXAFS oscillation frequencies increase with nearest-neighbor distances. The lower curve in Figure 1 shows our experimental data. The match to the $d_{\perp} = 1.55\text{\AA}$ calculation reported previously⁷ is evident. The registry of the selenium layer with the nickel surface was

found to be relatively unimportant in determining the calculated result:¹³ nearly the same curve was obtained for different local site geometries, if they were compared at the same d_{\perp} .

Empirically, NPD data thus behave similarly to EXAFS data with the important difference that the structural sensitivity is to d_{\perp} rather than R_{nn} . In the context of investigating this analogy further, we report in this paper new temperature-dependence results on the Se-Ni(001) model system. Taken at face value, these data are of interest in further characterizing the system. Of more general interest, however, is their value in characterizing the NPD phenomenon: in fact they constitute more evidence for the NPD-EXAFS analogy.

Section II includes some experimental information. Section III presents data that establish two forms of p(2x2) "Se" on Ni(001) and emphasizes the importance of accumulating an extended k-space data set. In Section IV we report a study of the temperature dependence of NPD data. Section V includes a summary and some conclusions.

II. Experimental

Experiments were performed on the 4° branch of Beam Line I at the Stanford Synchrotron Radiation Laboratory. The photoemission spectrometer and our technique for generating NPD data have been described elsewhere.¹⁴ The stored ring current was rather low

during these experiments (11-14 mA), but our spectrometer's multi-channel detection capability allowed experiments to be performed readily. Complete spectra around the Se(3d) peak were collected at each photon energy, to permit accurate corrections for background and for energy-dependent resolution.

The nickel crystal, which was oriented to within 1° of the (001) face, had previously been cleaned of bulk impurities so that only minor amounts of argon ion etching followed by annealing at 600°C were necessary to produce a clean and ordered surface. Initially, carbon, usually the most tenacious surface impurity, could not be detected using Auger electron spectroscopy, but a small carbon (1s) peak was visible using photoemission at $h\nu = 360$ eV, a photon energy where the carbon (1s) level has a reasonably large cross-section. It appears that, at least in our apparatus, the C(1s) sensitivity by photoemission is significantly better than by Auger spectroscopy. We suspect from this experience that minor carbon contamination ($< .05$ monolayers) is more prevalent in studies of this surface than the literature tends to imply. A subsequent, more extensive etching-annealing procedure followed by a fairly rapid quenching of the sample was found to produce a contaminant-free surface. Ordered $c(2 \times 2)$ and $p(2 \times 2)$ selenium coverages were produced by directing an effusive beam of H_2Se at the clean surface. In the experiments described in section IV, the surface was heated during exposure to $\sim 200^\circ\text{C}$, and 20-30 Langmuir exposures were sufficient to produce sharp $c(2 \times 2)$ overlayers. The $p(2 \times 2)$ coverages of section III

required 7-10 Langmuirs, but the surface was initially not heated, as explained below. The ambient chamber pressure was 4×10^{-10} Torr, and all surface preparations were observed to be stable for several hours.

III. Two forms of p(2x2) "Se"/Ni(001): The importance of an extended data range

The importance of accumulating EXAFS data as far above the edge as possible is well known and has been emphasized in several places.^{15,16} In Fourier transforming EXAFS data, a contribution to the real space peak widths of $\Delta r \sim \pi/\Delta k$ is introduced by the necessarily finite range of k over which EXAFS oscillations are observable.¹⁷ This broadening at least partially limits the accuracy and resolution of the EXAFS technique. In light of our comments in the introduction, a similar effect should be important in NPD.

Figure 2 shows two different NPD data sets accumulated at $T = 120\text{K}$ for the p(2x2) Se-Ni(001) system. The upper curve was accumulated using an unannealed overlayer prepared by exposing to H_2Se at 120K, while the lower curve was accumulated after an anneal at 450K. Both surfaces yielded p(2x2) LEED patterns, though that of the annealed surface was sharper. While the same general structure is observed in the curves, a systematic and monotonically increasing shift of peak positions to lower energy is evident in the

upper curve. The amplitude of oscillation is also larger in the lower curve. The data in that curve are in good agreement with our previous data,⁷ and are best fitted as before by a calculated curve with $d_{\perp} = 1.55\text{\AA}$, corresponding to the accepted four-coordinated hollow site adsorption geometry. The most likely explanation for the shifts observed in the upper curve is that d_{\perp} has increased slightly, leading to slightly more rapid oscillations. Since the higher-energy peaks disperse more rapidly with d_{\perp} , the higher energy regions are further out of phase. Indeed, if we had limited our study to $h\nu \leq 160$ eV, the pronounced shift seen in Figure 2 would have been difficult to discern. The lesson is the same as in EXAFS: an extended data range permits more accurate and higher resolution NPD studies.

An estimate can be made of the magnitude of the change in d_{\perp} by two independent methods. The calculations by Tong and Li¹³ over a wide range show that the fourth and fifth peaks in Figure 2 disperse with d_{\perp} at average rates of ~ 60 and ~ 80 eV/ \AA . Combining this with the shifts indicated in Figure 2 yields $\Delta d_{\perp} \approx 0.1\text{\AA}$.

Another estimate can be made as follows. Assume that the relationships

$$E_p = Ak_p^2$$

$$d_{\perp} = B/k_p$$

apply qualitatively to the kinetic energy (E_p) and wave number (k_p) to the peaks in our NPD curves, and to the distance parameter d_{\perp} .

It is easy to show that a small shift in d_{\perp} is given by

$$\Delta d_{\perp} = -d_{\perp} (\Delta E_p / 2E_p)$$

if E_p is measured from a suitable origin and ΔE_p is the shift in peak energies. This yields $\Delta d_{\perp} = 0.06\text{\AA}$ for the upper curve in Figure 2, in fair agreement with the above estimate of 0.1\AA .

Now the observed energy shift ΔE is very easy to resolve in this case, implying that our sensitivity in d_{\perp} is much better than $0.06\text{-}0.1\text{\AA}$, and certainly substantially better than the $\pm 0.1\text{\AA}$ typical of LEED studies. Indeed, its localized nature and phase coherence should make the ultimate precision (and perhaps accuracy) of NPD as high as that of EXAFS ($\pm 0.01\text{\AA}$).^{15,16} Considering the complexity of PD calculations relative to an EXAFS data analysis, however, it is not clear whether such accuracies can be attained in practice.

Several factors mitigate against covering such wide data ranges in NPD studies. Analyzer transmission functions generally decrease at higher kinetic energies. Also, in the soft x-ray regime, the usual problems of monochromator flux, resolution, and scattered light become more severe at higher energies. These experimental problems are the primary constraints on our present experimental efforts. They will, however, probably be overcome with the introduction of new synchrotron radiation facilities and monochromator designs. In addition to these practical constraints, there are also some fundamental limitations on the range of useful data, familiar from EXAFS. Temperature effects become more pronounced at higher

energies (see Section IV), and the scattering cross-sections are monotonically decreasing functions of energy.¹⁵⁻¹⁸ Both of these effects reduce the amplitude of oscillation relative to the atomic background. Finally, the atomic photoemission cross-section decreases at higher energies. While all of these effects make the quest for extended-data-range-NPD studies appear difficult, in fact these constraints are either surmountable or the same as those in EXAFS. Considering that NPD oscillations are at least a factor of ten larger than EXAFS oscillations, we feel that higher-energy NPD studies are quite possible.

Our observation of a shift in d_1 in this system is interesting in its own right. It tends to imply that H_2Se does not dissociate on a cooled Ni(001) surface. If so, there are at least two "chemical" reasons for an increase in d_1 . The first is simply a steric effect: the added bulk of the hydrogens precludes selenium atoms from fitting as far down into the fourfold hollow site. There should also be an electronic effect. Nickel is energetically stabilized by receiving electrons, thus filling its d-shell. The presence of hydrogen bonded to the selenium atoms will lessen the ability of selenium to donate electrons, producing a weaker and perhaps longer nickel-selenium bond.

IV. The temperature dependence of NPD oscillations.

In the last section, it was pointed out that thermal disorder is expected to limit the energy range over which useful NPD data

may be accumulated. In order to investigate this point more fully, we have undertaken a detailed study of the temperature dependence of NPD data for the $c(2 \times 2)$ Se-Ni(001) system. In the simplest model, one would expect some combination of the temperature sensitivities of LEED and EXAFS to affect NPD data. One expects the usual thermal diffuse scattering of LEED and x-ray diffraction to degrade the NPD final state in much the same way as it destroys the contrast of LEED beams.¹⁸ In addition, the electron source in NPD is itself vibrating, causing a distribution of d_{\perp} 's to contribute to the NPD result. This is analogous to the effect of temperature on EXAFS data, where a distribution of bond lengths causes the amplitude of oscillation to decrease.^{15,16} In view of several theories which predict substantially enhanced vibrations of the outermost surface layer relative to those typical of bulk layers,¹⁹⁻²² this latter effect might be expected to make NPD (and SEXAFS) experiments somewhat more sensitive to temperature than LEED.

Most thermal diffuse scattering mechanisms are interpreted in terms of a Debye-Waller factor:^{17,18}

$$I \sim \exp - \langle (\Delta \vec{k} \cdot \Delta \vec{r})^2 \rangle$$

which diminishes the fraction of coherently scattered particles. Assuming a Debye model for vibrational frequencies and amplitudes, and also that the vibrations are isotropic, this equation is reduced to the form familiar from x-ray diffraction studies:^{17,18}

$$I \sim \exp - \left(\frac{3|\Delta\vec{k}|^2 T}{m k_B \Theta^2} \right) \quad (1)$$

with m = the atomic mass, k_B = Boltzmann's constant, T = the absolute temperature, and Θ = the Debye temperature. This functional form is such that thermal effects are most pronounced at high energy and temperature. It has been found empirically that LEED intensities are exponential in temperature, but that Θ is a function of $\Delta\vec{k}$, indicating that the assumptions involved (Debye model) and multiple scattering preclude accurate applications of the simple model.¹⁸ On the other hand, EXAFS data have been shown theoretically²³ and experimentally²⁴ to follow this simple functional form. It will be interesting to ascertain the extent to which a simple model such as this can treat NPD data.

We have accumulated NPD curves for the $c(2 \times 2)$ Se-Ni(001) system at various temperatures above and below room temperature. Three data sets are shown in Figure 3 for $T = 300\text{K}$, 500K , and 700K . Only the region between $130 \text{ eV} \leq h\nu \leq 210 \text{ eV}$ photon energy was accumulated in most of our curves, to speed data acquisition. This is the energy region where one partial wave²⁵ dominates the atomic excitation step and also where the atomic background is smooth.²⁶ These points will be important later. The effect of increased temperature is apparent in Figure 3: the amplitude of oscillation decreases significantly at higher temperatures.

To treat the data, we wish first to isolate the scattering

contribution by producing an EXAFS-like plot of $(I-I_0)/I_0$, where I_0 is a smooth atomic background. Liebsch showed¹ that such a separation is not rigorously meaningful in general for initial states other than s-levels, due to interference between the two outgoing partial wave components of the final state. Such a separation, however, is a good approximation for a 3d level in this particular energy range, where the $d \rightarrow f$ channel dominates.^{25,26} In practice, the separation is still not completely straightforward. Fortunately, the general results we will derive are not particularly sensitive to the exact technique one chooses to use, provided the curves are treated consistently. All of our curves, when superimposed and scaled, intersect to within 1-2 eV of photon energies $h\nu = 142, 159, 186, \text{ and } 210 \text{ eV}$. Hence, we assumed that scattering effects are negligible at these energies and determined I_0 as a smooth curve through those points which also smoothly joins the high and low energy data at selected temperatures. The resulting plots of I_0 , shown as dashed curves in Figure 3, actually resemble one another closely, providing a good self-consistency check. Plots of $(I-I_0)/I_0$ are shown in Figure 4 for these three temperatures, and a pronounced temperature effect is again observed.

In Figure 5, we show the dependence of $\ln((I-I_0)/I_0)$ on temperature for the two photon energies corresponding to the two peaks in Figure 3. Aside from substantial random scatter, an approximately linear plot is obtained. The functional form of Eq.(1) is therefore obeyed, although the Debye model per se is inappropriate.

It is instructive to replace θ in Eq. (1) by an effective temperature θ_{eff} , then use it to fit the data. If effective temperatures are derived from the slopes of linear least squares fits to the data at the two peak energies, the results are $\theta_{\text{eff}} = 135\text{K}$ and 133K for photon energies of 149 and 192 eV, respectively. A consistent, but probably less accurate, value of $\theta_{\text{eff}} = 125\text{K}$ was derived from the amplitude of the minimum at $h\nu = 174$ eV.

These results deserve several comments. First, the linearity of the plots suggest that some simple model might explain the temperature dependence. Of course, logarithmic plots are not very sensitive to details of the functional form of the temperature variation of NPD amplitude, and to infer that a Debye-Waller factor explains our data would be premature. Second, the effective temperatures are rather low compared to typical bulk Debye temperatures of nickel. This is consistent with, but does not prove, enhanced surface vibrational motion. It does prove the importance of not underestimating thermal diffuse scattering in NPD. Finally, and perhaps most important, the effective temperatures for the two peak photon energies are, within statistical errors, identical. Further work is needed to determine over what energy range this final conclusion is valid, but it lends further credence to the concept of an effective temperature θ_{eff} describing thermal diffuse scattering in NPD.

V. Summary and Conclusions

We have reported temperature-dependent NPD studies. Several empirical similarities between NPD and EXAFS were noted. The two

techniques are complementary in their structural sensitivities, yielding d_{\perp} and R_{nn} , respectively. A combined surface EXAFS-NPD experiment would be of interest. It is remarkable that EXAFS, an angle- and energy-integrated technique, and NPD, an angle- and energy-resolved technique, should possess such qualitative similarities. The characteristic shift of NPD peaks with d_{\perp} has always indicated to us that some theoretical framework might be applicable which is simpler than the LEED formulations currently in use in treating NPD data. If the temperature dependent NPD data we have presented are typical, they provide further evidence that such a simple model exists. The immediate conclusion from this work is that NPD efforts will benefit from extended data ranges acquired from cooled surfaces. We are also led to suggest a search for a simpler theoretical framework in which NPD data may be interpreted.

ACKNOWLEDGMENTS

We wish to acknowledge Max G. Mason for his assistance in carrying out some of the measurements, and Mrs. Winifred Heppler for the preparation of the nickel crystals.

This work was performed by the Division of Chemical Sciences, Office of Basic Energy Sciences, U.S. Department of Energy under Contract No. W-7405-Eng-48. It was performed at the Stanford Synchrotron Radiation Laboratory, which is supported by the NSF Grant No. DMR 77-27489, in cooperation with the Stanford Linear Accelerator Center.

REFERENCES

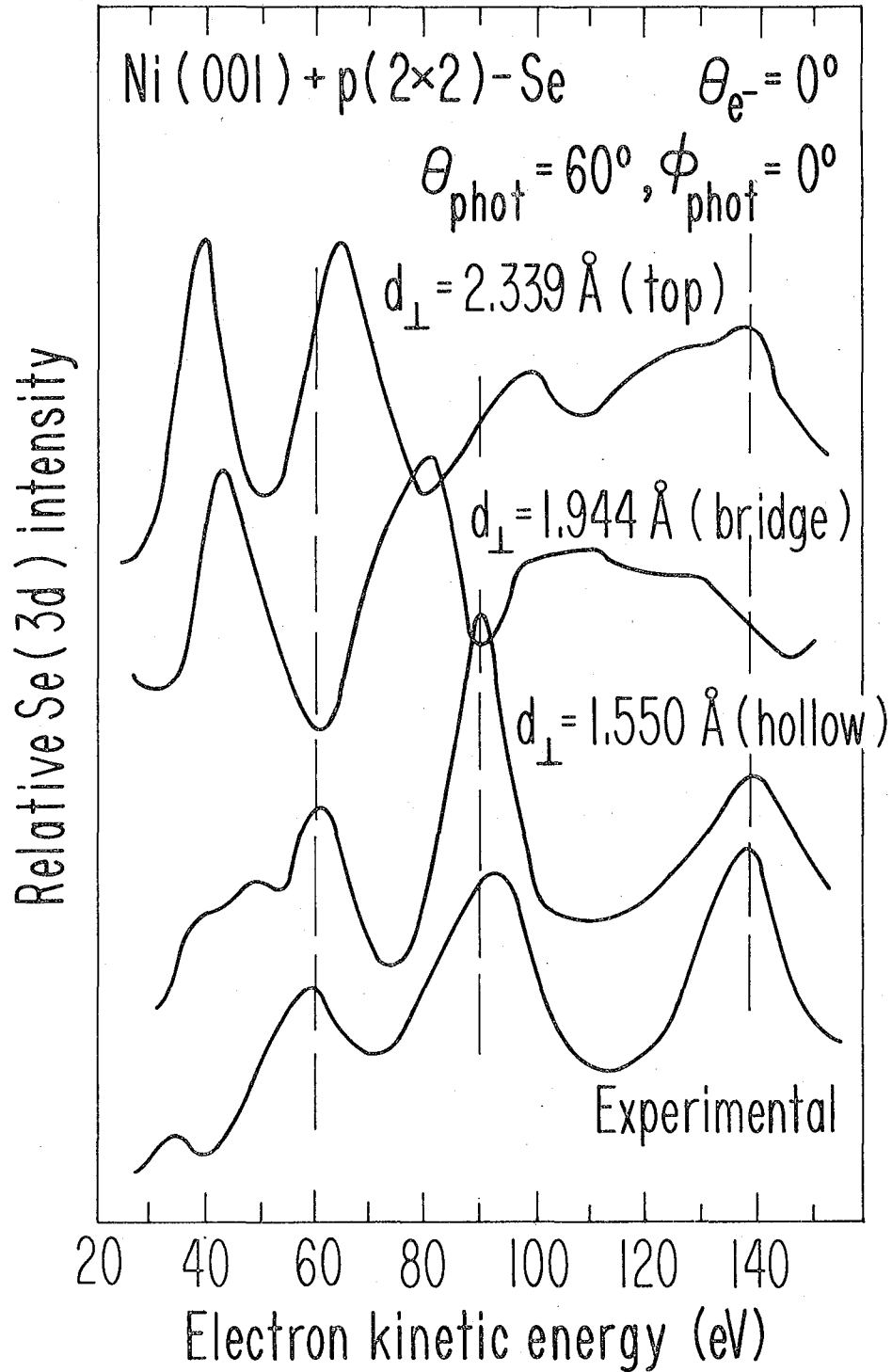
1. A. Liebsch, Phys. Rev. Lett. 32, 1203 (1974); Phys. Rev. B 13, 544 (1976).
2. I. Adawi, Phys. Rev. 134, A788 (1964).
3. P.J. Feibelmann and D.E. Eastman, Phys. Rev. B 10, 4932 (1974).
4. C.H. Li, A.R. Lubinsky, and S.Y. Tong, Phys. Rev. B 17, 3128 (1979).
5. J.B. Pendry, Surf. Sci. 57, 679 (1976); J. Phys. C 8, 2413 (1975).
6. B.W. Holland, J. Phys. C 8, 2679 (1975).
7. S.D. Kevan, D.H. Rosenblatt, D. Denley, B.-C. Lu, and D.A. Shirley, Phys. Rev. Lett. 41, 1565 (1978); Phys. Rev. B 20, 4133 (1979).
8. G.P. Williams, F. Cerrina, I.T. McGovern, and G.J. Lapeyre, Sol. State Commun. 31, 15 (1979).
9. D. Norman, D.P. Woodruff, N.V. Smith, M.M. Traum, and H.H. Farrell, Phys. Rev. B 18, 6789 (1978); D.P. Woodruff, D. Norman, B.W. Holland, N.V. Smith, H.H. Farrell, and M.M. Traum, Phys. Rev. Lett. 41, 1130 (1978); N.V. Smith, H.H. Farrell, M.M. Traum, D.P. Woodruff, D. Norman, M.S. Wolfson, B.W. Holland, Phys. Rev. B 21, 3119 (1980).
10. S. Kono, C.S. Fadley, and Z. Hussain, Phys. Rev. Lett. 41, 117 (1978); S. Kono, S.M. Goldberg, N.F.T. Hall, and C.S. Fadley, Phys. Rev. Lett. 41, 1831 (1978).

11. E.A. Stern, Phys. Rev. B 10, 3027 (1974).
12. P.A. Lee and J.B. Pendry, Phys. Rev. B 11, 2795 (1975).
13. C.H. Li and S.Y. Tong, Phys. Rev. B 19, 1769 (1979).
14. S.D. Kevan, Ph.D. thesis, University of California, Berkeley (1980), unpublished.
15. E.A. Stern, D.E. Sayers, and F.W. Lytle, Phys. Rev. Lett 27, 1204 (1971); Phys. Rev. B 11, 4836 (1975).
16. T.M. Hayes, P.N. Sen, and S.H. Hunter, J. Phys. C 9, 4357 (1976).
17. B.E. Warren, X-Ray Diffraction, (Addison-Wesley, Reading, MA, 1969).
18. J.B. Pendry, Low Energy Electron Diffraction, (Academic Press, New York 1974).
19. L. Pietronero and E. Tosatti, Solid State Commun. 32, 255 (1979).
20. T. Matsubara and K. Kamiya, Prog. Theor. Phys. 58, 767 (1977).
21. T. Matsubara, Y. Iwase, and A. Momokita, Prog. Theor. Phys. 58, 1102 (1977).
22. J.Q. Broughton and L.W. Woodcock, J. Phys. C 11, 2743 (1978).
23. V.V. Schmidt, Bull. Acad. Sci. USSR, Ser. Phys. 25, 988 (1961); 27, 392 (1963).
24. J.D. Hanawalt, Z. Phys. 70, 293 (1930), and Franklin Inst. 214, 569 (1932); F.W. Lytle, Developments in Applied Spectroscopy, (Plenum, New York 1963), Vol. 2, p. 285.

25. H.A. Bethe and E.E. Salpeter, Quantum Mechanics of One and Two Electron Atoms, (Academic Press, New York 1957).
26. S.T. Manson, Advances in Electronics and Electron Physics 44, 1 (1977); F. Combet Farnoux, J. Phys. (Paris) 32, (C4), 227 (1972).

Figure Captions

- Figure 1. Top three curves: calculated selenium 3d intensity as a function of electron kinetic energy for p(2x2) Se-Ni(001) at three different values of d_{\perp} as defined in the text, after Tong and Li. Bottom curve: experimental result.
- Figure 2. Comparison of NPD curves for frozen and annealed p(2x2) Se-Ni(001). Note the systematic shift of peak energies.
- Figure 3. NPD results taken at three temperatures for the p(2x2) Se-Ni(001) system. Dashed lines indicate an approximate atomic background as explained in the text.
- Figure 4. Plots of $(I-I_0)/I_0$ for the three temperatures in Figure 3. Curves are smoothed versions of the real data.
- Figure 5. Plots of $\ln((I-I_0)/I_0)$ vs. absolute temperature for 149 and 192 eV photon energy.



XBL7911-13241

Figure 1

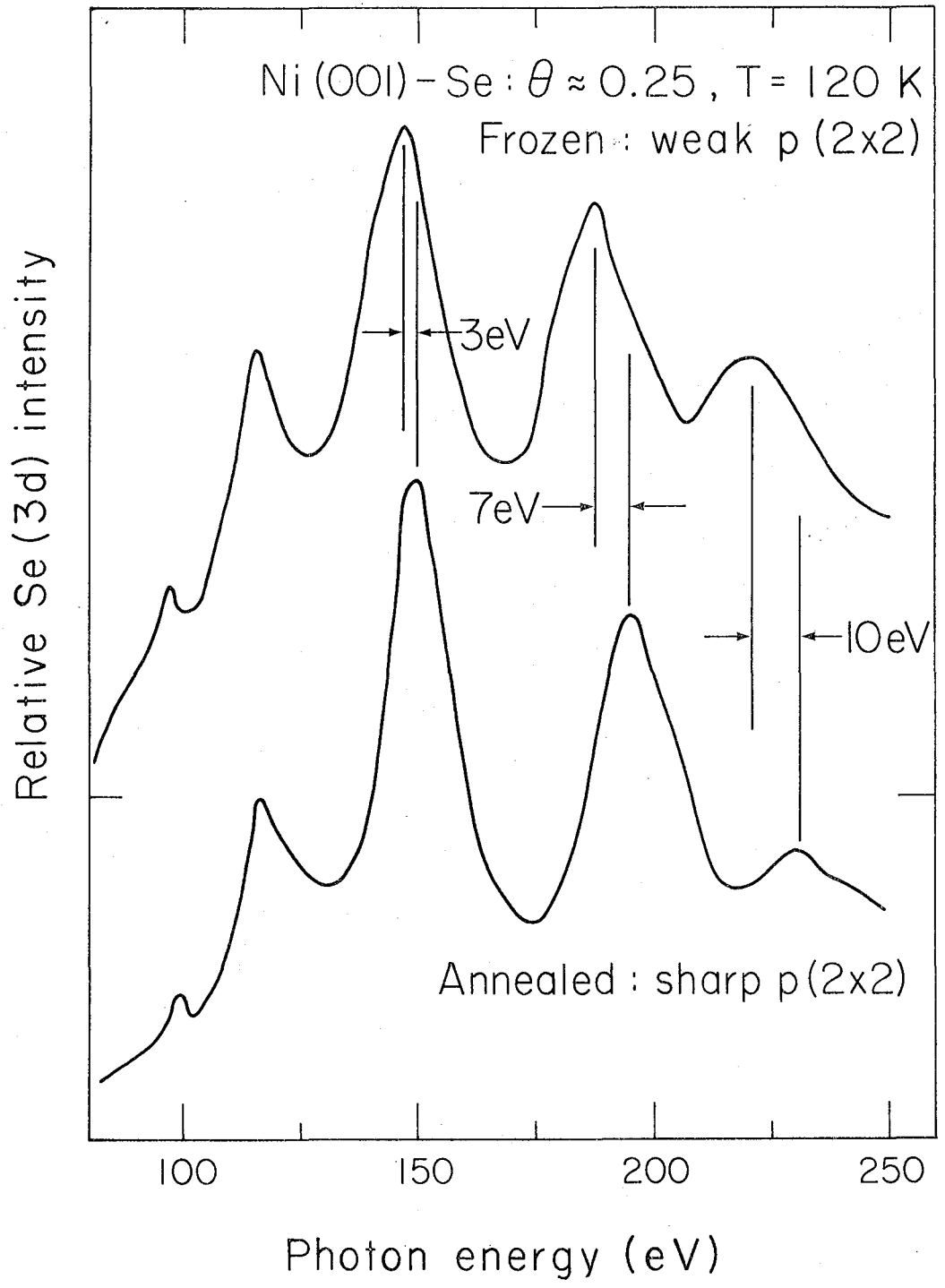


Figure 2

XBL805-1071

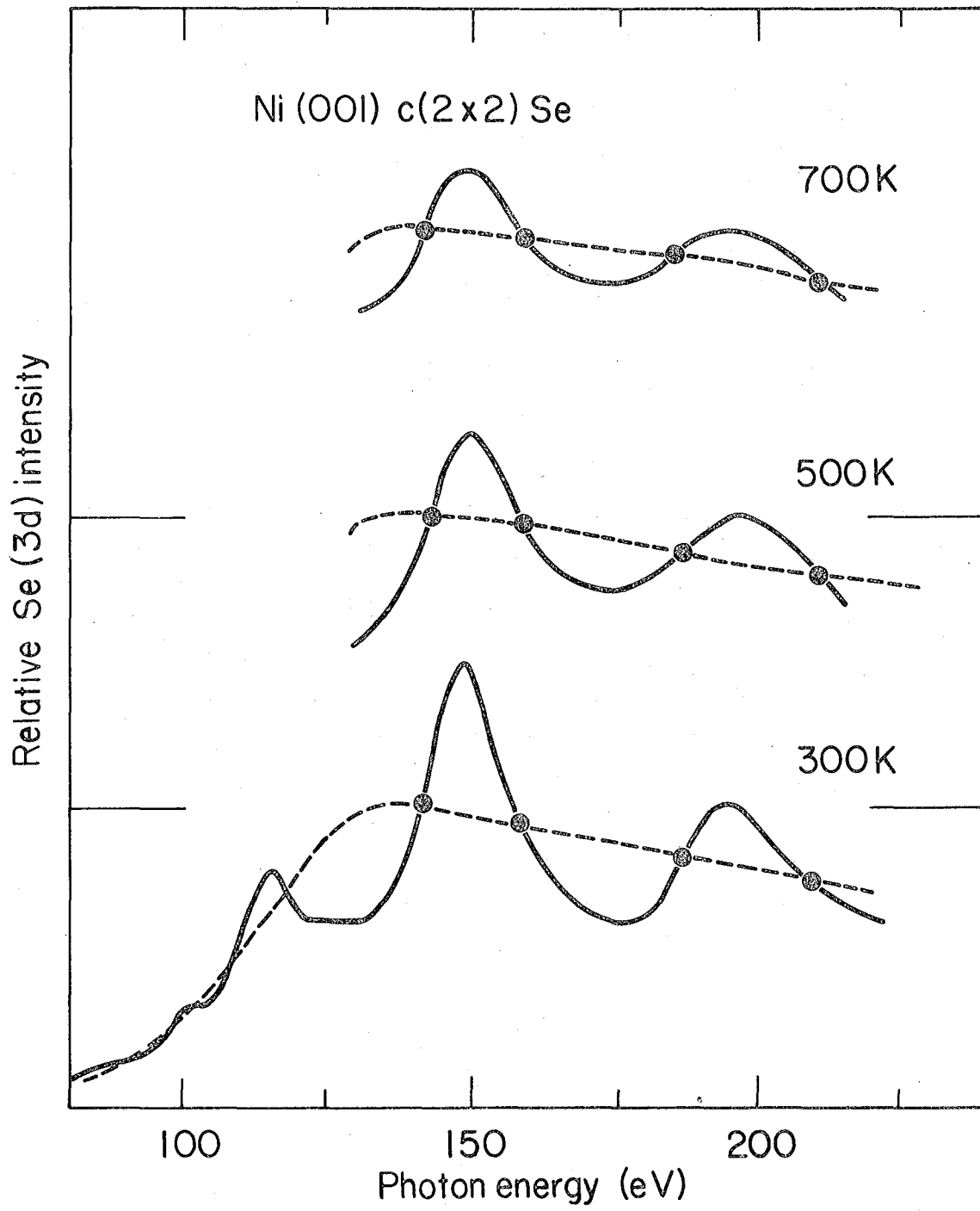


Figure 3

XBL-806-1360

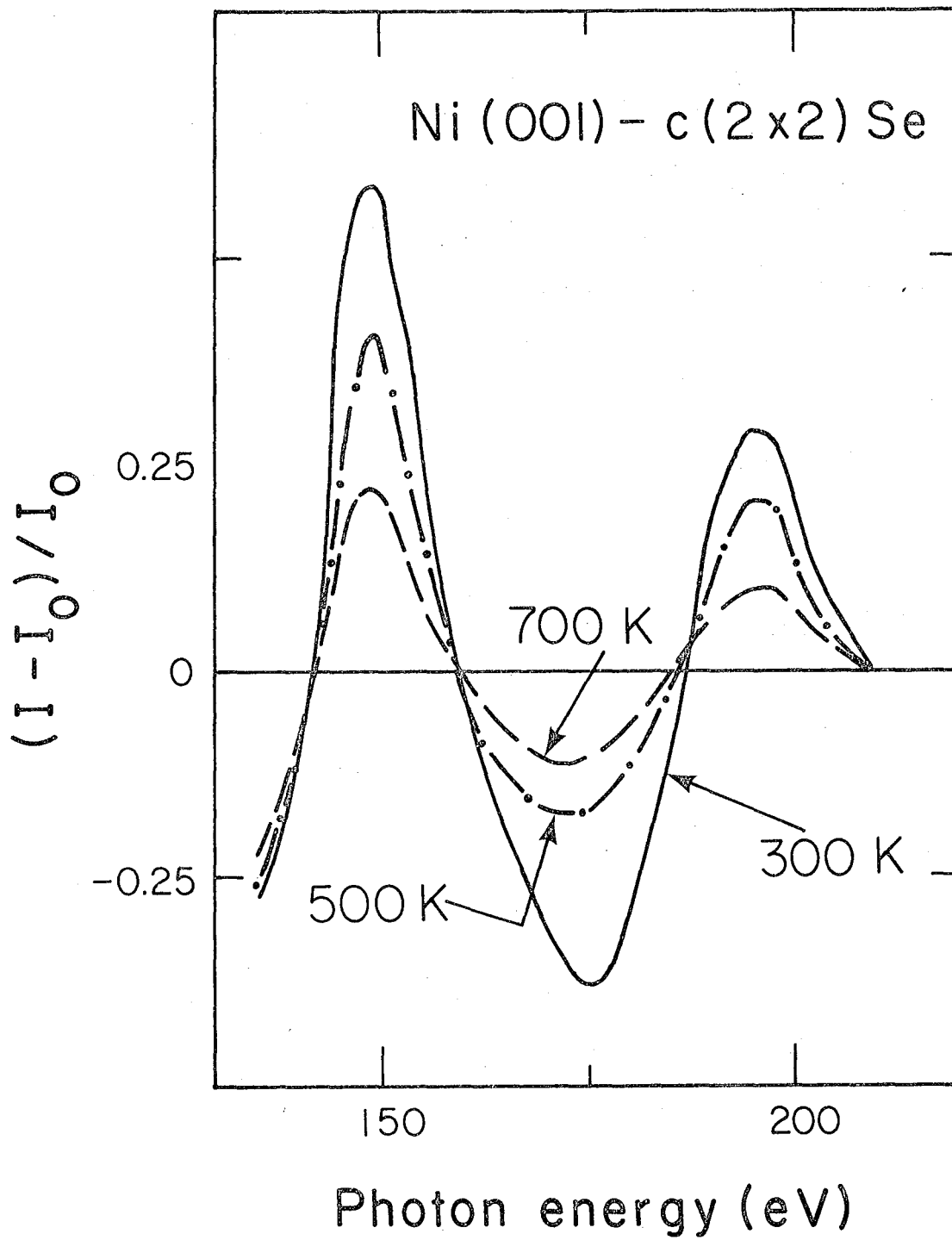
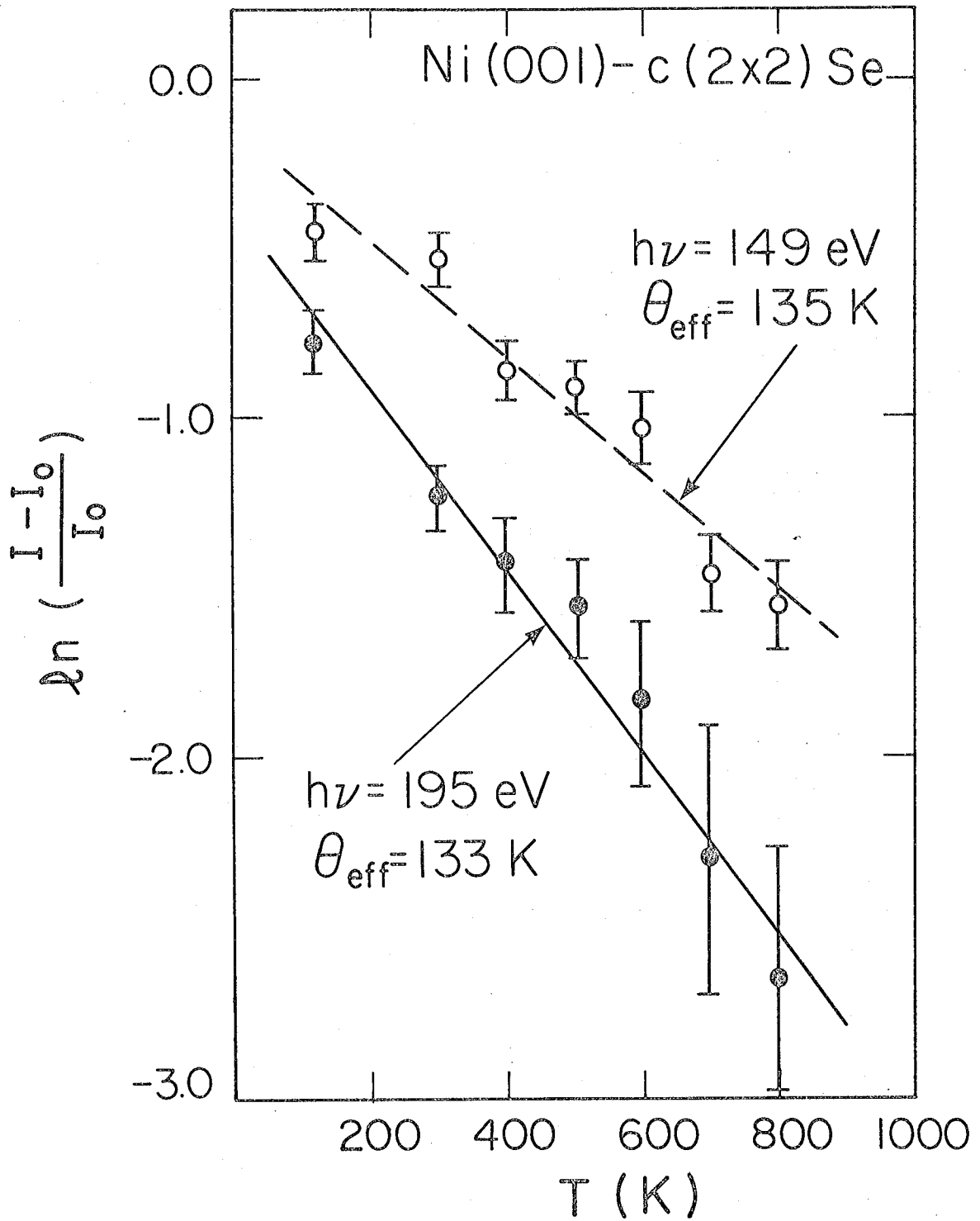


Figure 4

XBL 805-1072



XBL 805-1073

Figure 5

This report was done with support from the United States Energy Research and Development Administration. Any conclusions or opinions expressed in this report represent solely those of the author(s) and not necessarily those of The Regents of the University of California, the Lawrence Berkeley Laboratory or the United States Energy Research and Development Administration.